Particle detection and non-detection in a quantum time of arrival measurement

Denny Lane B. Sombillo, Eric A. Galapon

Theoretical Physics Group, National Institute of Physics, University of the Philippines, Diliman Quezon City, 1101 Philippines

Abstract

The standard time-of-arrival distribution cannot reproduce both the temporal and the spatial profile of the modulus squared of the time-evolved wave function for an arbitrary initial state. In particular, the time-of-arrival distribution gives a non-vanishing probability even if the wave function is zero at a given point for all values of time. This poses a problem in the standard formulation of quantum mechanics where one quantizes a classical observable and uses its spectral resolution to calculate the corresponding distribution. In this work, we show that the modulus square of the time-evolved wave function is in fact contained in one of the degenerate eigenfunctions of the quantized time-of-arrival operator. This generalizes our understanding of quantum arrival phenomenon where particle detection is not a necessary requirement, thereby providing a direct link between time-of-arrival quantization and the outcomes of the two-slit experiment.

Keywords: Quantum Mechanics, Quantum time of arrival, Wave function collapse, Two-slit experiment

1. Introduction

Time of arrival (TOA) has always been associated with particle appearance [1]. This is the reason why attempts to construct a quantum TOA distribution uses particle detection as its primary assumption [2, 3, 4, 5, 6, 7]. Now, the probability of finding a particle in the neighborhood of X at an instant of time t is already encapsulated in the position density distribution $|\psi(X,t)|^2$. If particle detection is indeed necessary for quantum arrival, then the TOA distribution should resemble both the temporal and spatial profile of the time-evolved position density. Following the standard formulation of quantum mechanics, a TOA operator can be obtained by quantizing the classical TOA. The spectral resolution of the quantum TOA operator can then be used to generate the TOA distribution for a given initial state. Such distribution is often referred to as the standard TOA distribution [25, 26]. However, the standard TOA distribution fails to give the correct temporal and spatial profile of the time-evolved position density for an arbitrary initial state. This is due to the suppression of the interference arising from the positive and negative momentum components of the initial state [9, 10]. We are now confronted with the following problems: Is the standard formulation (i.e. quantization of classical observable followed by spectral analysis) wrong? If not, then what does the quantized TOA operator actually measures? Is it still possible to consistently extract the time-evolved position distribution from the standard TOA distribution? This paper will address these questions.

In this work, we will show that the position distribution is indeed contained in the standard quantum TOA distribution and that the quantum arrival has a broader meaning than the classical particle detection phenomenon. We will first examine a specific case when the standard TOA fails to give the correct spatial and temporal profile of the time-evolved position distribution. Using the properties of the confined time-of-arrival (CTOA) operator, we were able to isolate the term in the unconfined standard TOA distribution that correspond to particle appearance. In the end, we will learn that the quantization of the classical TOA give rise to a quantum phenomenon which is at the very core of quantum mechanics, i.e. the two-slit experiment.

In [12], one of us proposed that particle appearance is a consequence of TOA measurement. That is, the initial wave function of a particle collapses into one of the confined time of arrival (CTOA) operator eigenfunctions right after the preparation and evolve according to the Schrödinger equation [15, 16]. At the time equal to the CTOA eigenvalue, the evolving eigenfunction becomes a function with a singular support at the arrival point. The instant when the wave function has its minimum position uncertainty is interpreted as particle appearance in [12]. The proposed mechanism suggests that a quantum particle may be materialized via smooth unitary evolution in contrast to the abrupt collapse upon measurement. One can therefore infer a strong connection between the time-evolved position density and the TOA distributions. However, such connection was established only in the theory of

CTOA operator, which is still problematic in terms of operational interpretation [17]. In this paper, we intend to reconcile the time-evolved position and the more established standard TOA distributions in the fundamental level, i.e. without any reference to a detector. We will do this by exploiting the known properties of the CTOA operator such as the two distinct unitary arrivals.

This work is organized as follows. First, we show that the particle appearance interpretation can be extended to the unconfined case in section 2. In section 3, we compare the TOA distribution with the time-evolved position density for different initial states. This is followed by describing the relevant features of the CTOA theory in section 4 and using those features to extend the interpretation of the standard TOA in section 5. Then, we relate the reinterpreted TOA measurement with the two-slit experiment in section 6. Finally, we give our conclusion in section 8.

2. The Standard TOA Distribution

A TOA operator can be constructed for a non interacting case such that it satisfies the required canonical commutation relation with the free Hamiltonian. The standard TOA operator is given by $\hat{T} = -\mu[(\hat{q}-X)\hat{p}^{-1}+\hat{p}^{-1}(\hat{q}-X)]/2$, where X is the arrival point, μ is the mass of the particle, $\hat{q}$ is the position operator and $\hat{p}$ is the momentum operator [18]. The operator $\hat{T}$, though not self adjoint, is maximally symmetric and therefore can still be used to generate the desired distribution. The spectral resolution of $\hat{T}$ is obtained by solving the eigenvalue problem $\hat{T}\left|\tau\right\rangle = \tau\left|\tau\right\rangle$, where τ is the TOA eigenvalue and $\left|\tau\right\rangle$ is the corresponding eigenstate. The solution to the eigenvalue problem is easily facilitated in momentum representation, i.e.

$$-i\mu\hbar\left(\frac{1}{p}\frac{\partial}{\partial p}-\frac{1}{p^2}+i\frac{X}{\hbar p}\right)\left\langle p\right|\tau\rangle = \tau\left\langle p\right|\tau\rangle . \tag{1}$$

This admits the solution

$$\left\langle p\right|\tau_{\pm}^{X}\rangle = \sqrt{\frac{|p|}{\mu}}\frac{e^{-iXp/\hbar}}{\sqrt{2\pi\hbar}}\mathrm{e}^{i\tau p^2/2\mu\hbar}\Theta(\pm p), \tag{2}$$

where $\left\langle p\right|\tau_{\pm}^{X}\rangle$ are the degenerate eigenfunctions of $\hat{T}$ with eigenvalue τ and $\Theta(p)$ is the Heaviside function [8]. Given an initial state $\left|\psi_0\right\rangle$, one can construct the TOA density distribution via:

$$\Pi_{\psi_0}(X,\tau) = \left|\left\langle\tau_{+}^{X}\right|\psi_0\rangle\right|^2 + \left|\left\langle\tau_{-}^{X}\right|\psi_0\rangle\right|^2 \tag{3}$$

The first and second terms are associated with the particles moving rightwards and leftwards, respectively.

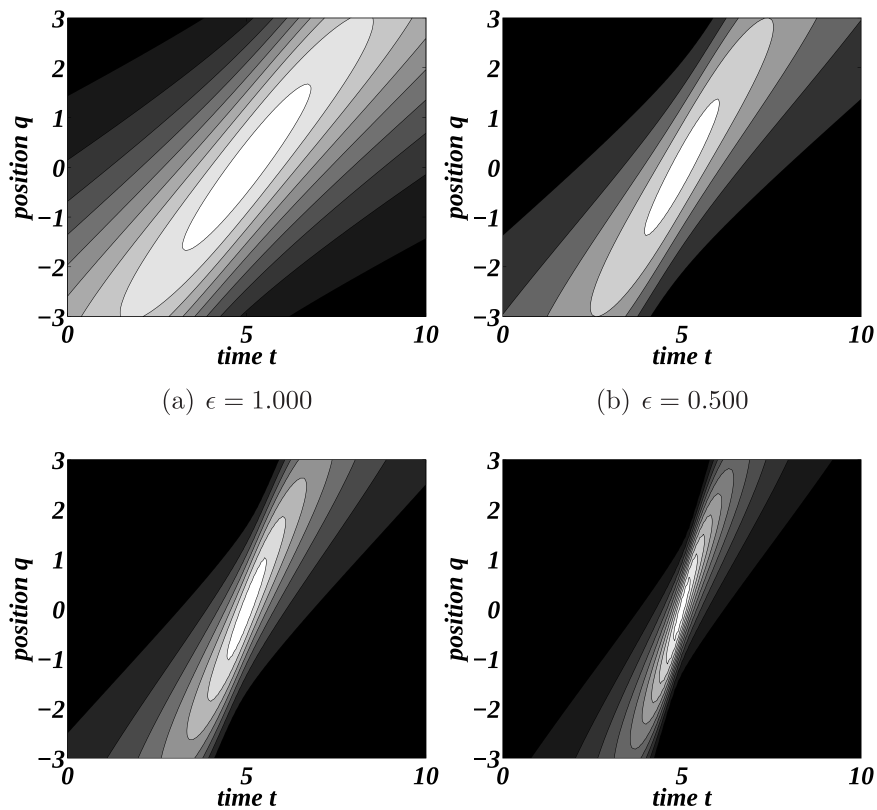

(a) $\epsilon = 1.000$ (b) $\epsilon = 0.500$

(c) $\epsilon = 0.250$ (d) $\epsilon = 0.125$

Figure 1: Time evolution of the standard quantum TOA operator eigenfunction distribution $\left|\left\langle q\right|\tau_+^X(t)\right\rangle\right|^2$ for decreasing ϵ. Lighter regions correspond to high probability density value while darker regions correspond to low density value. The arrival point is set to $X = 0$ and the time eigenvalue at $\tau = 5$. Similar dynamical behavior is obtained for $\left|\left\langle q\right|\tau_-^X(t)\right\rangle\right|^2$ (not shown).

Properties of the standard TOA operator eigenfunctions are explored in details in [23]. One important feature of the TOA eigenfunction is its unitary evolution. This is governed by the time development operator given by: $\hat{U}_t^K = \mathrm{e}^{-i\hat{p}^2 t/2\mu\hbar}$. To probe the dynamics of the standard TOA eigenfunctions, we evaluate the corresponding amplitude $\left\langle q\right|\tau_+^X(t)\right\rangle$ by integrating this in momentum space. Anticipating that the integral is divergent, we introduce a converging factor $\mathrm{e}^{-\epsilon p^2}$ such that

$$\begin{aligned}\langle q|\, U_t^K \,|\tau_+^X\rangle &= \lim_{\epsilon\to 0}\int_{-\infty}^{+\infty} dp\, \langle q|\, p\rangle\, \mathrm{e}^{-ip^2 t/2\mu\hbar}\, \langle p|\, \tau_+^X\rangle\, \mathrm{e}^{-\epsilon p^2} \\ &\propto \lim_{\epsilon\to 0}\int_{0}^{+\infty} dp \sqrt{\frac{|p|}{\mu}} \exp\left[\frac{(X-q)p}{i\hbar} + \frac{(t-\tau)p^2}{2i\mu\hbar}\right] \mathrm{e}^{-\epsilon p^2}.\end{aligned} \tag{4}$$

Notice that when we set the position q to be at X, the integral will become divergent as $\epsilon \to 0$ only when $t = \tau$. If we interpret a wave function with singular support at the arrival point $q = X$ to be a particle's appearance, then the time when this happens correspond to the particle's first arrival time. This means that the eigenvalue time τ of the standard TOA operator is the first time of arrival of a particle that is initially prepared in the corresponding eigenfunction. The dynamics are explcitly shown in Fig.1 for decreasing ϵ where the position distribution approaches a singular value at $q = X$ only in time $t = \tau$.

It turns out that the TOA operator eigenfunctions exhibit a particle-like collapse, i.e. they unitarily evolve into a wave function with singular support at time equal to the TOA eigenvalue. Thus, the interpretation that the appearance of particle is due to the TOA measurement holds for the unconfined case. Consequently, this means that we should be able to relate the particle's position probability density to the quantum TOA distribution.

3. Relating the quantum TOA distribution with the position distribution

The distributions $\Pi_{\psi_0}(X,\tau)$ and $|\psi(q,t)|^2$ are not equivalent to each other in a sense that they are answers to two different questions. In particular, the probability of finding the particle in a small interval dq at a given point q at an instant of time t is $P(q,dq;t) = |\psi(q,t)|^2\, dq$, while the probability that a particle will arrive at a point X in a small time interval $d\tau$ at time τ is $\bar{P}(\tau, d\tau; X) = \Pi_{\psi_0}(X,\tau)d\tau$. The former is a probability density in space at fixed instant of time t while the latter is a density in time evaluated at a fixed point in space X. These distributions are complementary to each other, i.e. one can be used to addressed what the other distribution cannot. Also, these distributions should be consistent with each other, i.e. if $|\psi(q,t)|^2 = 0$ at some point $q = X$ for all time t, then we expect that $\Pi_{\psi_0}(X,\tau) = 0$.

3.1. Initial state with compact support in the half momentum line

The relationship between the position density and the TOA distribution is straightforward for initial state having a compact support in the half momentum line. These are shown in Fig.2 and 3. In Fig.2, where the initial state is a single-peak Gaussian function with positive momentum support, both the temporal and spatial profile of the TOA distribution agrees with the time-evolved position density. We get the same observation in Fig.3 where the initial state is a linear combination of two Gaussian, both of which have positive momentum support.

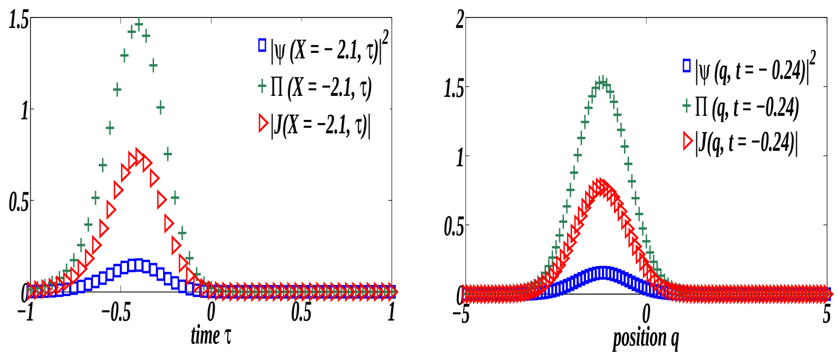

(a) (b)

Figure 2: Comparison of $|\psi(q,t)|^2$ (square) with $|J(X,\tau)|$ (triangle) and $\Pi_{\psi_0}(X,\tau)$ (cross) for fixed position (a) and fixed time (b). The initial state is given by $\psi_0(p) = \psi_+(p) = N\mathrm{e}^{-(p-p_0)^2/(4\sigma_p^2)}$ where N is a normalization constant and $p_0 > 0$.

The corresponding amplitudes are related via:

$$\begin{aligned} \left\langle \tau_+^X \middle| \psi_0 \right\rangle &= \int_{-\infty}^{+\infty} dp \frac{e^{ipX/\hbar}}{\sqrt{2\pi\hbar}} \sqrt{\frac{|p|}{\mu}} e^{-ip^2\tau/2\mu\hbar} \psi_0(p) \\ &= \langle X \,|\, \hat{\Omega} \hat{U}_\tau^K \,|\, \psi_0 \rangle \end{aligned} \tag{5}$$

where we used $\langle X | p \rangle = e^{ipX/\hbar}/\sqrt{2\pi\hbar}$ and introduced the operator $\hat{\Omega} = \sqrt{|\hat{p}|/\mu}$. One will recognize that the vector $\hat{U}_\tau^K |\psi_0\rangle$ is the free evolving state $|\psi(\tau)\rangle$. Inserting the identity resolution of the position eigenstates in (5) we obtain the desired relationship between the two amplitudes

$$\left\langle \tau_+^X \middle| \psi_0 \right\rangle = \int_{-\infty}^{+\infty} dq \, \langle X \,|\, \hat{\Omega} \,|\, q \rangle \, \psi(q,\tau). \tag{6}$$

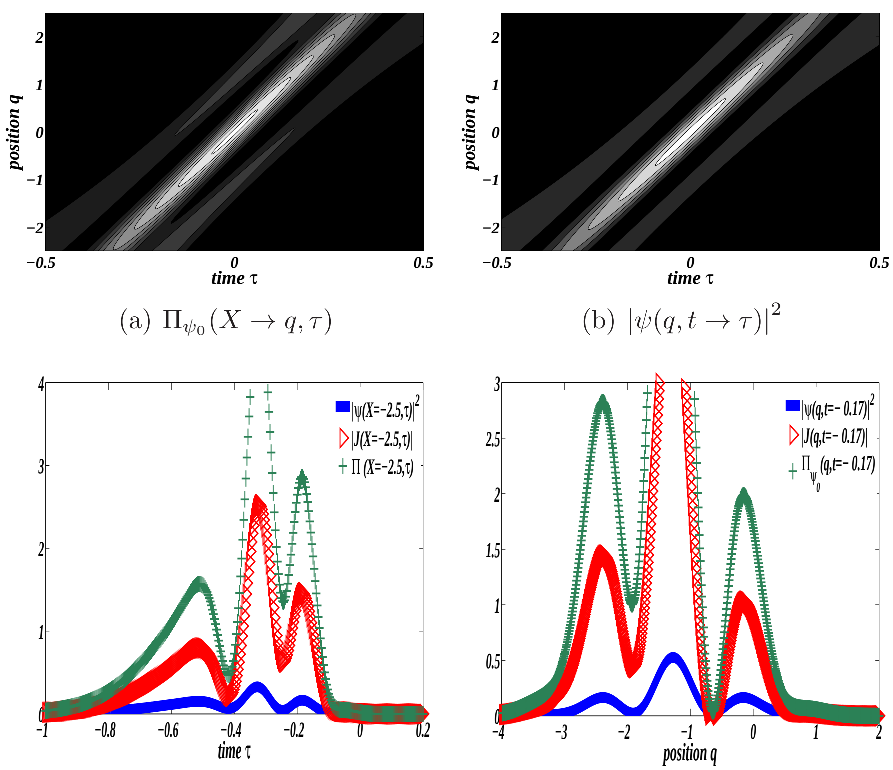

(a) $\Pi_{\psi_0}(X \rightarrow q, \tau)$ (b) $|\psi(q, t \rightarrow \tau)|^2$

(c) (d)

Figure 3: Contour plots of unnormalized distributions $\Pi_{\psi_0}(X \rightarrow q, \tau)$ (a) and $|\psi(q, t \rightarrow \tau)|^2$ (b) for initial state $\psi_0(p) = N[\psi_{1+}(p) + \psi_{2+}(p)]$ where $\psi_{n+}(p) \propto e^{-(p-p_n)^2/(4\sigma_p^2)}$ with $p_2 > p_1 > 0$. The distribution $|J(X \rightarrow q, \tau)|$ (not shown) is similar to (a). The profiles of the three distributions are shown in (c) for fixed position slice and in (d) for fixed time slice.

The left side of (6) contains the amplitude of the standard TOA distribution while the right side contains the amplitude of the time evolved position distribution. This relationship is reminiscent of the crossing states discussed in [13, 14]. We can also invert the process by expanding the amplitude $\langle q | \hat{U}_t^K | \psi_0 \rangle$ in terms of the identity resolution of the TOA eigenstates, i.e.

$$\langle q | \psi(t) \rangle = \sum_{\sigma=\pm} \int_{-\infty}^{+\infty} d\tau_\sigma^X \langle q | \hat{U}_t^K \left| \tau_\sigma^X \right\rangle \left\langle \tau_\sigma^X \right| \psi_0 \rangle . \tag{7}$$

Note that only the $\sigma = +$ will contribute to the expansion due to the restriction that we put on $|\psi_0\rangle$, i.e. $\langle p | \psi_0 \rangle$ has a compact support only in the positive momentum line.

3.2. Initial state with positive and negative momentum components

So far, the relationships that we have established are only valid when the initial state has a compact support in the half momentum line. Let us consider a more general case, i.e. when the initial state has both negative and positive momentum components.

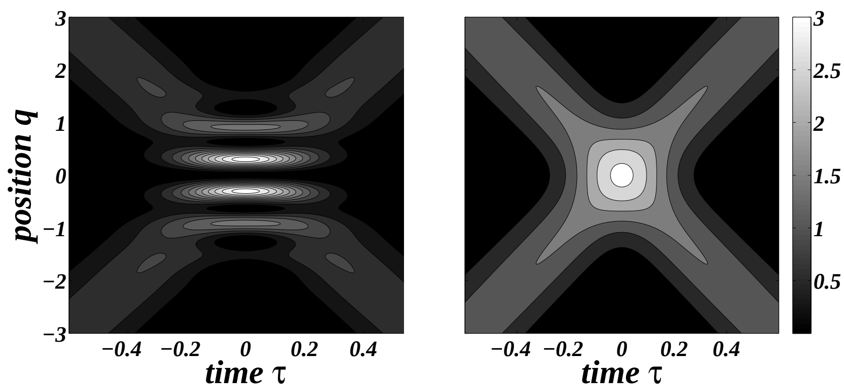

(a) $|\psi(q, t \to \tau)|^2$ (b) $\Pi_{\psi_0}(X \to q, \tau)$

Figure 4: The time-evolved position density distribution (a) and the position-scanned standard TOA distribution (b). The initial state used is the antisymmetric $\psi_0(p) = N(\psi_+(p) - \psi_-(p))$, where $\psi_\pm(p) = \mathrm{e}^{-(p \pm p_0)^2/(4\sigma_p^2)}$ and N is a normalization constant.

Previous works on the TOA distribution are always associated with initial wave function that has either positive or negative momentum but not both. This is to ensure that the particle will appear at the arrival point after some time. Under this framework, the identity resolution of the TOA operator takes the form

$$\mathbb{I} = \int_{-\infty}^{+\infty} d\tau \left(\left|\tau_+^X\right\rangle\left\langle\tau_+^X\right| + \left|\tau_-^X\right\rangle\left\langle\tau_-^X\right| \right) \tag{8}$$

and is physically interpreted that the particle will arrive sooner or later [9, 23, 24]. However, nothing in the formulation of the TOA operator restricts us in choosing our initial state.

Let $\langle p|\,\psi_0\rangle = \left[\psi_+(p)e^{ipq_+/\hbar} - \psi_-(p)e^{ipq_-/\hbar}\right]/\sqrt{2}$ be our initial antisymmetric state where $\psi_+(p)$ and $\psi_-(p)$ are functions with compact support in the positive and negative momentum values respectively with $\psi_-(-p) =$

$\psi_+(p)$. If we evaluate $\langle X | \hat{U}_\tau^K | \psi_0 \rangle$ and set $X = -(q_+ + q_-)/2$, we will obtain $\psi(X, \tau) = 0$ for all time τ. A vanishing wave function implies the non appearance of particle at that given point. We expect the TOA distribution to exhibit the same result at $X = -(q_+ + q_-)/2$. However, if we evaluate $\Pi_{\psi_0}(X, \tau)$ using this antisymmetric initial state, we will get a non zero finite probability value. This is explicitly illustrated in Figure 4 where the horizontal dark line corresponding to fixed value of q, i.e. $|\psi(q = 0, \tau)|^2 = 0$ in Fig. 4(a), are in fact not dark in Fig.4(b) for $\Pi_{\psi_0}(X = 0, \tau)$. The observed interference in the time-evolved position density did not manifest in the standard TOA distribution. The suppression of the interference term in $\psi(q, \tau)$ is due to the forced separation of the positive and negative momentum components of $\psi_0(p)$ in (2).

3.3. Probability current and the time-evolved position density

The problem on the absence of interference in the standard TOA was already recognized by Leavens in [25, 10]. He contends that the association of arrivals from left or right with positive or negative momentum respectively is not justified. In addition, for a particular antisymmetric initial state, Leavens was able to show that the probability current $|J(X, \tau)| = (\hbar/\mu)\mathrm{Im}(\bar{\psi}\partial_q\psi)|_{q=X}$ agrees with the vanishing of the wave function for all time τ. Such agreement is observed directly when the initial state has a compact support in the half momentum line (Fig.2 and Fig.3). Does this favor the proposed use of probability current to calculate the TOA distribution over the standard operator approach (see for example [11])? If the answer to this question is in affirmative, then $|J(X, \tau)|$ should be able to reproduce the spatial and temporal profile of $|\psi(X, \tau)|^2$ for any initial state.

It turns out that $|\psi(X, \tau)|^2$ does not always agree with $|J(X, \tau)|$ if we treat the latter as a TOA distribution. This can be demonstrated by considering a symmetric combination of $\psi_+(p)$ and $\psi_-(p)$ as an initial state. We will find that the probability current vanishes for all τ at some X where $|\psi(X, \tau)|^2$ is not necessarily equal to zero. In fact, the probability current vanishes at $X = -(q_+ + q_-)/2$ for both the symmetric and antisymmetric initial states. The vanishing of the current for the antisymmetric initial state is due to $\psi(X, \tau) = 0$ while its vanishing for the symmetric case is due to $\partial_q\psi(q, \tau)|_{q=X} = 0$. This should not be surprising since for both the symmetric and antisymmetric combination of $\psi_+(p)$ and $\psi_-(p)$, the net flux of probability at X is always zero. The symmetric case shows that the appearance of particle at a given point does not necessarily require a non-vanishing current. This is further

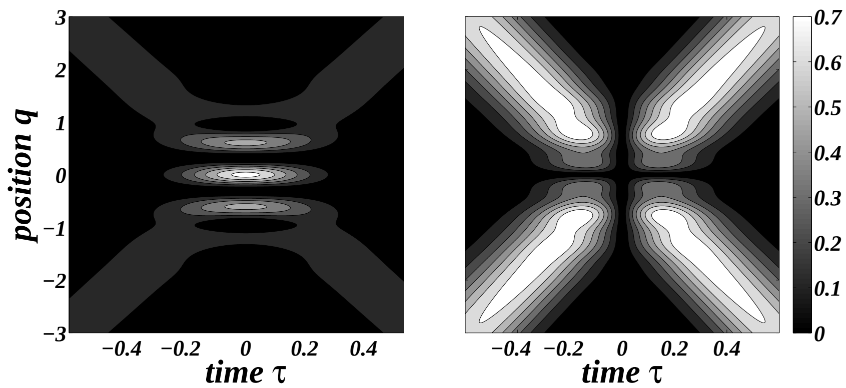

(a) $|\psi(q, t \to \tau)|^2$ (b) $|J(X \to q, \tau)|$

Figure 5: The time-evolved position distribution (a) and the probability current for different arrival point (b). The initial state used is the symmetric $\psi_0(p) = N(\psi_+(p) + \psi_-(p))$, where $\psi_\pm(p) = \mathrm{e}^{-(p \pm p_0)^2/(4\sigma_p^2)}$ and N is a normalization constant.

illustrated in Fig.5 where the peak of $|\psi(q,t)|^2$ at $q = 0$ corresponds to the zero probability current $|J(X = 0, \tau)|^2 = 0$ for all time τ. This disqualifies $|J(X, \tau)|$ as a legitimate way of calculating the TOA distribution if we insist that particle appearance is a necessary requirement for quantum arrival.

4. Revisiting the Confined Time of Arrival

We have seen that the link suggested by (6) and (7) breaks down when the initial state has both positive and negative momentum components. If the TOA distribution predicts a finite probability despite having a vanishing time-evolved wave function, then either the standard quantum TOA operator is wrong or it measures a time associated with a more general arrival phenomenon. The former poses a serious problem in the foundation of quantum mechanics, i.e. do we have to put an ad hoc assumption (in addition to the canonical commutation relation) whenever we quantize a classical observable? On the other hand, the latter gives us an avenue for further exploration. Some of the interesting questions that we can address are: What does the standard TOA operator actually measures? What new phenomenon do we get in quantizing a classical observable? The answers to these questions are revealed in the dynamics of the CTOA operator.

The standard TOA operator is maximally symmetric but not self-adjoint.

Though it is already sufficient in the construction of TOA distribution, it will be innocuous if one proceed to construct a self-adjoint version of standard TOA operator. The issue of self-adjointness was addressed via spatial confinement, i.e. confining the space into a segment $[-l, l]$ and by imposing the boundary condition $\varphi(-l) = e^{-2i\gamma}\varphi(l)$ for all $\varphi(q)$ in the system's Hilbert space [15, 16]. The confined time of arrival (CTOA) operator for the free particle case in position representation is a Fredholm integral operator $\hat{T}_\gamma \varphi(q) = \int_{-l}^{l} T_\gamma(q, q')\varphi(q')dq'$. The kernel is square integrable, i.e. $\int_{-l}^{l}\int_{-l}^{l} |T_\gamma(q, q')|^2 \, dqdq' < \infty$, which results into a compact operator $\hat{T}_\gamma$ having a complete set of eigenfunctions and discrete spectrum. It was shown in [17] that the CTOA approaches the standard TOA distribution in (3) as the confinement length is increased. This means that any observation that we have in the confined case could be extended to the unconfined case.

In the limit of large confinement length, the CTOA operator eigenfunctions become two-fold degenerate that are orthogonal to each other for a given arrival time eigenvalue. Unlike the standard TOA, the degenerate CTOA eigenfunctions are classified in terms of their parity about the arrival point. The eigenfunctions with even parity are called non-nodal while those with odd parity are referred to as nodal. These degenerate eigenfunctions arise naturally without any prior assumption of where the particle is coming from.

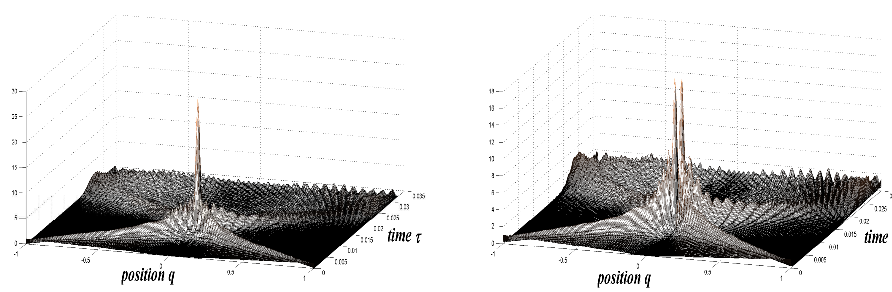

(a) non-nodal eigenfunction distribution (b) nodal eigenfunction distribution

Figure 6: Time-evolved distribution of the non-nodal 6(a) and the nodal 6(b) eigenfunctions of the free CTOA operator.

One noticeable feature of the CTOA operator eigenfunctions is their unitary dynamics. In Fig.6, both the evolution of the nodal and the non-nodal eigenfunctions exhibit unitary collapse, i.e. their position uncertainty becomes a minimum at a time equal to the CTOA eigenvalue [15, 16]. In contrast to the evolution of the standard TOA eigenfunctions in Fig.1, two different dynamics are observed in Fig.6. The non-nodal eigenfunctions exhibit the same behavior as that of Fig.1, where it becomes a distribution with a singular support at the arrival point at a time equal to the CTOA eigenvalue. Such unitary collapse is amenable to particle appearance interpretation. It follows that the overlap of the initial state with one of the CTOA non-nodal eigenstate gives the probability amplitude that the particle will appear at the arrival point with a minimum position uncertainty.

It would be mistaken, however, to extend the same interpretation to the case of nodal dynamics in Fig.6(b). The reason is that the nodal eigenfunction is zero at the arrival point for all time t despite having a minimum position uncertainty at the eigenvalue time. So how do we interpret the nodal eigenfunctions dynamics? This will be answered in the next section.

5. Quantum Arrival with Particle Appearance

Let us go back to the standard TOA operator that is defined in the entire real line. We can construct a set of nodal and non-nodal eigenfunctions for the standard TOA operator by superposing the result in (2) such that the resulting function in position representation has a certain parity about the arrival point. Note that the equal superposition of (2) is still an eigenfunction of the standard TOA operator with the same eigenvalue. Specifically, if we let $\bar{\phi}(p)$ be the momentum representation of a function $\phi(q)$ with certain parity about $q = X$, i.e. $\phi(X - q) = \pm\phi(X + q)$, then one can show that $e^{ipX/\hbar}\bar{\phi}(p)$ is either odd or even about $p = 0$. For $p \neq 0$, the alternative set of degenerate eigenfunctions are

$$\begin{aligned}\left\langle p\right| \tau_{non}^{X}\rangle &= \sqrt{\frac{|p|}{2\mu}}\frac{e^{-ipX/\hbar}}{\sqrt{2\pi\hbar}}e^{ip^2\tau/2\mu\hbar} \\ \left\langle p\right| \tau_{nod}^{X}\rangle &= \sqrt{\frac{|p|}{2\mu}}\frac{e^{-ipX/\hbar}}{\sqrt{2\pi\hbar}}e^{ip^2\tau/2\mu\hbar}\cdot \mathrm{sgn}(p)\end{aligned} \tag{9}$$

where $\left|\tau_{non}^{X}\right\rangle$ and $\left|\tau_{nod}^{X}\right\rangle$ are the non-nodal and the nodal eigenstates of the standard TOA operator, respectively, with the same eigenvalue τ. If we evolve (9) in time, we will get a similar behavior as that shown in Fig.6.

Using the alternative set of eigenfunctions, the standard TOA distribution becomes

$$\Pi_{\psi_0}(X,\tau) = \left|\left\langle \psi_0 \right| \tau^X_{non} \right\rangle\right|^2 + \left|\left\langle \psi_0 \right| \tau^X_{nod} \right\rangle\right|^2 . \tag{10}$$

The non-nodal contribution correspond to particle appearance at the arrival point and therefore, it should agree with the time-evolved position distribution. This can be verified by comparing the first term of (10) with $|\psi(q,t)|^2$. Similarly, the meaning of the nodal unitary collapse in Fig.6(b) can be interpreted by comparing the second term of (10) with $|\psi(q,t)|^2$.

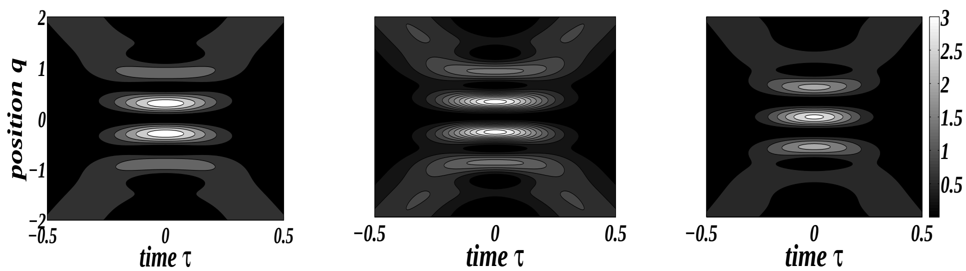

(a) non-nodal (b) $|\psi(q,t)|^2$ (c) nodal

Figure 7: Comparison of the non-nodal and nodal TOA distributions with the time-evolved position density distributions. The initial state used is the antisymmetric $\psi_0(p) = N(\psi_+(p) - \psi_-(p))$, where $\psi_\pm(p) = \mathrm{e}^{-(p\pm p_0)^2/(4\sigma_p^2)}$ and N is a normalization constant.

Figures 7(a) and 7(b) shows the non-nodal TOA distribution and the time-evolved position distribution, respectively, for an anti-symmetric initial state. Notice that the peaks in Fig.7(a) correspond to the peaks of Fig.7(b). This supports the interpretation that the non-nodal contribution corresponds to quantum arrival with particle appearance. We also compare the time-evolved position distribution in Fig.7(b) with the nodal TOA distribution in Fig.7(c). In contrast to the non-nodal case, the point where $|\psi(q,\tau)|^2 = 0$, i.e. at $q = 0$ for all time τ, corresponds to the maximum of the nodal distribution. This means that the nodal distribution is a maximum when there is no particle appearance. Now, being one of the degenerate eigenstate of the standard TOA operator, the nodal distribution implies that we have a quantum arrival with no particle appearance. Consequently, the dynamics of the degenerate eigenfunctions in Fig.6 correspond to two possible outcomes of a quantum TOA measurement, i.e. the appearance or the non-appearance of particle at the arrival point. This generalizes our notion of quantum arrival, i.e. the particle is not compelled to appear at the arrival point. In

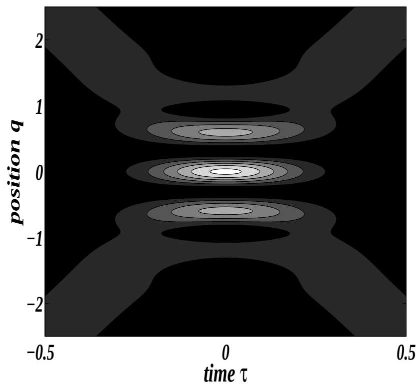

(a)

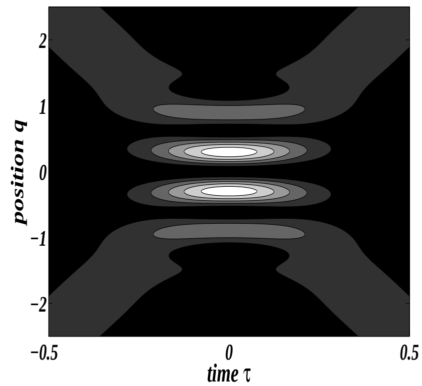

(b)

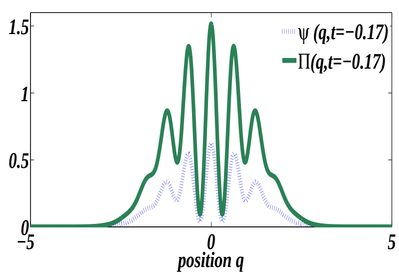

(c)

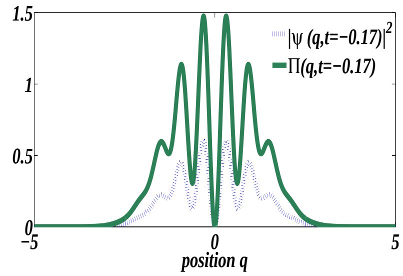

(d)

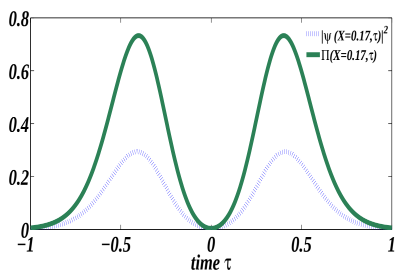

(e)

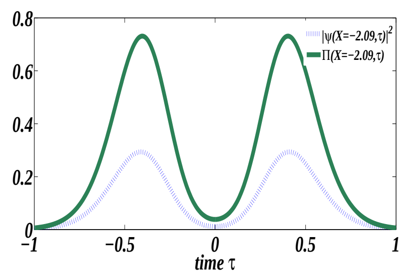

(f)

Figure 8: The non-nodal time of arrival distributions for the symmetric (a) and antisymmetric (b) initial state. The profiles of $\left|\left\langle \psi_0 \right| \tau_{non}^X \right\rangle\right|^2$ is compared to $|\psi(q,t)|^2$ for the fixed time and position for the symmetric case (c and e) and antisymmetric case (d and f).

particular, we can define the quantum arrival to be a phenomenon where the position uncertainty becomes a minimum at the arrival point. Both of the possibilities depicted in Fig.6 agree with this definition. Furthermore, given an initial state $|\psi_0\rangle$, we can assign a probability to each of the quantum arrival outcomes. If we multiply (10) with $d\tau$, then we can write

$$\begin{aligned} P_{\{X,\tau\}}(arrive) = P_{\{X,\tau\}}(arrive\ \cap\ appear) \\ + P_{\{X,\tau\}}(arrive\ \cap\ not\ appear) \end{aligned} \tag{11}$$

where $P_{\{X,\tau\}}(arrive)$ gives the probability that the particle will quantum mechanically arrive at X in a small time interval containing τ. The probabilities $P_{\{X,\tau\}}(arrive\ \cap\ appear)$ and $P_{\{X,\tau\}}(arrive\ \cap\ not\ appear)$ are the respective joint probabilities that correspond to the two possible outcomes of a quantum TOA measurement.

If one is only interested in TOA measurement with particle detection, then the relevant probability should come from the non-nodal eigenstates, i.e.

$$P_{\{X,\tau\}}(arrive\ \cap\ appear) = \left|\left\langle \psi_0 \right| \tau^X_{non} \right\rangle\right|^2 d\tau \tag{12}$$

where $\left|\left\langle \psi_0 \right| \tau^X_{non} \right\rangle\right|^2$ is the quantum TOA distribution associated with particle appearance. This is further demonstrated in Fig.8 where the non-nodal TOA distributions are calculated for two different initial states. Figures 8(c) and 8(e) shows the temporal and the spatial profile agreement between the non-nodal TOA distribution and the time-evolved position distribution for the symmetric initial state. Figures 8(d) and 8(f) shows how the temporal and the spatial profile of the non-nodal TOA distribution matches with $|\psi(q,t)|^2$ for the anti-symmetric initial state.

One can check that (10) is equivalent to (3) via the transformation $\left|\tau^X_{non}\right\rangle = (|\tau_+\rangle + |\tau-\rangle)/\sqrt{2}$ and $\left|\tau^X_{nod}\right\rangle = (|\tau_+\rangle - |\tau-\rangle)/\sqrt{2}$. However, the terms that appear in each distribution describe different events. Both terms in eq.3 correspond to particle appearance with minimum position uncertainty at the arrival point as shown in Fig.1, one is coming from the left and the other is coming from the right. In eq.10, the first and second term corresponds to particle appearance and non-appearance, respectively, both with minimum position uncertainty at the arrival point (Fig.6). The two sets of degenerate eigenfunctions of the standard TOA has a repercussions in our understanding of temporal quantization. It turns out that the two set of TOA eigenfunctions, i.e. the right/left and nodal/non-nodal, correspond to the outcomes of the two-slit experiment in one dimension. This will be the subject of the next section.

6. TOA eigenfunctions and the two-slit experiment

The arrival set-up that we are considering so far is similar to the two-slit experiment with two possible paths, i.e. particle can either be coming from the left or the right with respect to the arrival point. If we know which path the particle came from, then the resulting pattern on the screen is a characteristic of a particle. This is similar to the behavior of the right and left moving eigenstates of the standard TOA operator. Either of these eigenstates guarantee a particle appearance at the arrival point as illustrated in Fig.1. However, if we have no prior knowledge of the particle's path, then the pattern on the screen exhibit a wave-like nature, i.e. we can either have a destructive or a constructive interference. Particle appearance is no longer guaranteed. This is similar to the nodal and the non-nodal eigenstates of the TOA operator where particle appearance is only possible for the non-nodal case as shown in Fig.6. It turns out that if we treat the two-slit experiment as a TOA measurement, then knowing the particle's path collapses the initial state into either the left/right moving eigenstates or into nodal/non-nodal eigenstates of the TOA operator.

The momentum distribution of the initial state determines the set of eigenfunctions that will come into play in a TOA measurement. If the initial state has a compact support in the half momentum line, then the initial state can only collapse into either the right or left moving eigenfunctions of the standard TOA operator. Otherwise, if the momentum support of the initial state has a positive and negative contributions then the state can collapse into either the non-nodal or the nodal TOA eigenstates. The former always give rise to particle appearance while the latter can result into either appearance (constructive interference) or non-appearance (destructive interference) of the particle at the arrival point. Our knowledge of the initial state reflects our knowledge of the particle's path at least in the one-dimensional case.

We now go back to one of the questions that we raised earlier, i.e. what do we get in quantizing the classical TOA? It turns out that the quantization of the classical TOA gives us (using the words of Feynman) a "phenomenon which is impossible, absolutely impossible to explain in any classical way" [27], which is the two-path quantum arrival. This arrival phenomenon comes naturally by implicitly imposing the position-momentum commutation relation in the construction of a TOA operator. The result of the two-path experiment emerged as a consequence of TOA measurement and gives a direct connection between the experiment outcomes based on our knowledge of the path and the position-momentum commutation relation.

7. Final comment

The original introduction of the standard TOA operator and most of its variants draw some controversies. One notable criticism is due to Mielnik and Torres-Vega in [19]. They raised several fundamental questions on the construction of time operator within the standard framework of quantum mechanics. We have detected at least two major conceptual challenges that we believe can now be addressed using the generalized meaning of quantum arrival event. First is on the absence of interference in the standard TOA distribution. The second is on the role of a waiting detector on the free evolution of the initial wave function prior to particle appearance. We will devote this last section in addressing these problems.

The first problem will only persists if one hold on to the old notion that particle detection is synonymous with quantum arrival. We have shown that one can extract the interference of the wave function's free evolution from the standard TOA distribution. One, however, has to generalize the definition of a quantum arrival event, i.e. it is an event where the position uncertainty is a minimum in the neighborhood of the arrival point. This quantum event is further classified into two possible outcomes, i.e. one correspond to particle detection while the other corresponds to particle non-detection. Both of which are a result of the collapse of the initial wave function into the nodal and the non-nodal eigenstates of the standard TOA operator. The interference that we see in the wave function's evolution correspond only to the quantum arrival with particle appearance which is contained in the standard TOA distribution. The interesting feature of the standard TOA distribution is that it contains the null result of an arrival measurement, signifying that there is also a temporal collapse even if we have a non-detection.

The second question can be addresed by generalizing the interpretation made in [12]. We will consider two different measurement schemes. The first one is we prepared the system initially, i.e. the particle and the detector, with an absolute intention to measure the particle's arrival. Without loss of generality, we will assume that the particle's initial wave function has a positive momentum support. Note that the particle will only be detected if its wave function evolves unitarily to become a function with a singular support at the arrival point for some time $t = \tau$. This will only happen if the particle is in one of the standard TOA operator eigenstates at time $t = 0$.

This implies that the initial state must collapse into one of the eigenfunctions of the standard TOA operator right after the preparation. The collapse will be followed by the free unitary evolution of the TOA operator eigenfunction until it becomes a wave function with a localized support in the neighborhood of the arrival point. If the localized wave function is non-vanishing at the arrival point, then we have a particle detection and the arrival time can recorded. Thus, the effect of a waiting detector is to collapse the initial state into one of the TOA eigenfunctions right after the preparation and that the particle detection is a consequence of the eigenfunction's unitary evolution.

Consider now the second mesurement scheme. We start with the same arrival time measurement set-up but decide to defer the TOA measurement. One might argue that our previous interpretation is incompatible with the second set-up for we expect to see a distribution (of the other non-TOA observable) that agrees with the time-evolved wave function. This means that the initial wave function should not collapse into one of the standard TOA eigenfunctions and just proceed to evolve unitarily. However, this apparent paradox does not exist because quantum mechanics is inherently non-local in time [22, 21, 20]. This means that the collapse into one of the TOA eigenfunctions right after the preparation (when a TOA measurement is to be made) and the Schrödinger's evolution of the initial wave function right after the preparation (when some other measurement is to be made) are two mutually exclusive potentialities that are simultaneously true for the system. Which possibility will be realized depends on the decision that we do to the system at the moment. We refer the reader to [12] for a more detailed explanation.

8. Conclusion

Our analysis shows that particle detection or appearance in a TOA measurement is just a special case of a more general quantum TOA phenomena. The quantization of the classical TOA expression, which we always associate with particle appearance, gives us an operator with eigenfunctions that evolve unitarily into a distribution with minimum position uncertainty. The state of minimum position uncertainty does not necessary imply a particle appearance for there are also state with the same feature that are vanishing at the arrival point. Thus, if we are going to restrict ourselves to particle detection as a requirement of arrival then we should only consider the non-nodal eigenstates of the TOA operator.

Our insight here is restricted only to the free-case where the parity of the standard TOA eigenfunctions plays an important role in qualifying the two possible outcomes of a quantum TOA measurement. Nevertheless, one can extend our analysis to the interacting case since previous works on the CTOA reveals a similar nodal and non-nodal unitary collapse [28].

Acknowledgments

D.S. acknowledges the Office of the Chancellor of the University of the Philippines Diliman, through the Office of the Vice Chancellor for Research and Development, for funding support through the Thesis and Dissertation Grant (Project No. 151503 DNSE). This work was supported by the Department of Science and Technology through the National Research Council of the Philippines.

References

[1] A.M. Steinberg in *Time in Quantum Mechanics* I eds. J.G. Muga, R.S. Mayato and I.L. Egusquiza, p. 333-353 (2008).

[2] A. Ruschhaupt, J.G. Muga and G.C. Hegerfeldt, in *Time in Quantum Mechanics* II eds. J.G. Muga, A. Ruschhaupt and A. Campo, p. 65-96 (2009).

[3] B. Navarro, I. L. Egusquiza, J. G. Muga, G. C. Hegerfeldt, *J. Phys. B* **36**, 3899 (2003).

[4] J. A. Damborenea, I. L. Egusquiza, G. C. Hegerfeldt, J. G. Muga, *Phys. Rev. A* **66**, 052104 (2002).

[5] J.J. Halliwell, *Prog. Theor. Phys.* **102**, 707-717 (1999).

[6] C. Anastopoulos, and N. Savvidou, *Phys. Rev. A* **86**, 012111 (2012).

[7] S. Dhar, S. Dasgupta and A. Dhar *J. Phys. A* **48**, 115304 (2015).

[8] R. Giannitrapani *Int. J. Theor. Phys.* **36**, 1575 (1997).

[9] I. L. Egusquiza, J. G. Muga, B. Navarro and A. Ruschhaupt *Phys. Lett. A* **313**, 498 (2003).

[10] C.R. Leavens *Phys. Lett. A* **345**, 251 - 257 (2005).

[11] N. Vona, G, Hinrichs, D. Dürr, *Phys. Rev. Lett.* **111**, 220404 (2013).

[12] E. A. Galapon *Proc. R. Soc. A* **465**, 71-86 (2009).

[13] A. D. Baute, R. Sala Mayato, J. P. Palao, J. G. Muga, and I. L. Egusquiza, *Phys. Rev. A* **61**, 022118 (2000).

[14] A. D. Villanueva, E.A. Galapon, *Phys. Rev. A* **82**, 052117 (2010).

[15] E. A. Galapon, R. Caballar and R. Bahague *Phys. Rev. Let.* **93**, 180406 (2004).

[16] E. A. Galapon, R. Caballar and R. Bahague *Phys. Rev. A* **72**, 062107 (2005).

[17] E. A. Galapon, F. Delgado, J. G. Muga and I. Esgusquiza *Phys. Rev. A* **72**, 042107 (2005).

[18] Y. Aharonov and D. Bohm *Phys. Rev.* **122**, 1649 (1961).

[19] B. Mielnik and G. Torres-Vega *Concepts Phys.* **2**, 81 (2005).

[20] J. Wheeler in *Mathematical foundations of quantum theory* ed. A.R. Marlow , p. 9-48 (1978).

[21] J. Wheeler in *Quantum theory and measurement* eds. J. Wheeler and W.H. Zurek, p. 182-203 (1984).

[22] Y.Aharonov and M.S. Zubairy *Science* **307**, 875-879 (2005).

[23] J. G. Muga, C. R. Leavens and J. P. Palao *Phys. Rev. A* **58**, 4336-4344 (1998).

[24] I. L. Egusquiza and J. G. Muga *Phys. Rev. A* **61**, 0121048 (1999).

[25] C. R. Leavens *Phys. Lett. A* **303**, 154-165 (2002).

[26] J.G. Muga and C.R. Leavens *Phys. Rep.* **338**, 353-438 (2000).

[27] Feynman, R., Leighton, R. and Sands, M. *The Feynman Lectures on Physics* Vol. III, Addison-Wesley (1963).

[28] E. A. Galapon *Int. J. Mod. Phys. A* **21**, 6351-6381 (2006).